Time-Domain modeling of saturation in conformal mapping approach for Permanent Magnet Synchronous Machines

Martin Hafner, David Franck and Kay Hameyer
Institute of Electrical Machines – RWTH Aachen University
Schinkelstraße 4, D-52062 Aachen, Germany
E-mail: Martin.Hafner@IEM.RWTH-Aachen.de

***Abstract*— In the electromagnetic field simulation of modern servo drives, the computation of higher time and space harmonics is essential to predict torque pulsations, radial forces, ripple torques and cogging torque. Field computation by conformal mapping (CM) techniques is a time-effective method to compute the radial and tangential field components. In the standard CM approach, computational results of cogging torque simulations as well as overload operations observe deviations to nonlinear finite element simulations due to the neglection of slot leakage and saturation effects. This paper presents an extension of the classical CM. Additional CM parameters are computed from single FE computations so as to consider both effects listed above in the model over a wide operation range of the electrical drive. The proposed approach is applied to a surface permanent magnet synchronous machine, and compared to numerical results obtained by FEA. An accuracy similar to that of FE simulations is obtained with however the low computation time that is characteristic for analytical models.**

I. Standard Conformal Mapping

The air gap field computation by conformal mapping is generally obtained from the solution of a linear Laplace problem, assuming the magnetic core has an infinite permeability. Since this system is linear, the field excitation by magnets and coils, as well the influence of the slotting, can be modeled individually.

Assuming a slotless stator, the field $\vec{B}(\Theta)$ at a certain coordinate angle Θ in the air gap, $\Theta \in [0, 2\pi[$, consists of a radial flux density $B_r(\Theta)$ and a tangential flux density $B_\varphi(\Theta)$

$$\vec{B}(\Theta) = B_r(\Theta) \cdot \vec{e}_r + B_\varphi(\Theta) \cdot \vec{e}_\varphi. \tag{1}$$

The angle dependent quantities $B_r(\Theta)$ and $B_\varphi(\Theta)$ can be expanded into a Fourier Series

$$\vec{B}(\Theta) = \sum_{n=0}^{\infty} \left(B_{r,n} \cdot \vec{e}_r + B_{\varphi,n} \cdot \vec{e}_\varphi\right) e^{\jmath np\Theta}, \tag{2}$$

where n is the frequency order and p the number of pole pairs. In this representation of the air gap field, the Fourier coefficients $B_{r,n}$ and $B_{\varphi,n}$ are the solution of a linear Laplace problem with magnets and a slotless stator depending on the magnetization configuration [1], [2], [3]. The field at a certain instance of time t due to rotor movement is given by

$$\vec{B}(t) = \vec{B} \cdot e^{\jmath\omega_r t} \tag{3}$$

where ω_r is the angular speed of the rotor.

Stator slotting significantly influences the magnetic field distribution. It is modeled by "permeance functions". These permeance functions $\vec{\lambda}$ represent the impact of slotting on the slotless field distribution and can be obtained by Schwarz-Christoffel transformations [4], [5]. Correlating the field distribution with slotting, ${}^{s}\vec{B}(t)$, with the field without slotting (3), yields the vectorial permeance $\vec{\lambda}$

$$\begin{aligned} {}^{s}\vec{B}(t) &= \vec{\lambda}^* \cdot \vec{B}(t) && (4)\\ \vec{\lambda}^* &= \begin{pmatrix} \lambda_r & \lambda_\varphi \\ -\lambda_\varphi & \lambda_r \end{pmatrix}. && (5) \end{aligned}$$

The air gap field excited by the armature current is given by

$${}^{a}\vec{B}(t, I, \psi) = \begin{pmatrix} {}^{p}\vec{B}\left(\sqrt{2}Ie^{\jmath(\omega_s t+0^\circ)}\right) \\ {}^{p}\vec{B}\left(\sqrt{2}Ie^{\jmath(\omega_s t+120^\circ)}\right) \\ {}^{p}\vec{B}\left(\sqrt{2}Ie^{\jmath(\omega_s t+240^\circ)}\right) \end{pmatrix} \cdot \begin{pmatrix} e^{\jmath(\phi_q+\psi+0^\circ)} \\ e^{\jmath(\phi_q+\psi+120^\circ)} \\ e^{\jmath(\phi_q+\psi+240^\circ)} \end{pmatrix}, \tag{6}$$

where ${}^{p}\vec{B}$ is the normalized field due to one phase and also obtained by conformal mapping [6]. In (6) the angle ϕ_q defines the relative phase orientation to the quadrature axis of the machine, ψ is the flux weakening angle and ω_s is the stator current angular frequency. We shall in the sequel systematically omit the coordinate Θ and the time argument t, and only indicate the dependency in I and ψ when applicable. We shall also label the quantities obtained by the conformal mapping approach with a CM exponent. The overall air gap field is thus defined as

$${}^{g}\vec{B}^{CM}(I, \psi) = {}^{a}\vec{B}^{CM}(I, \psi) + {}^{s}\vec{B}^{CM}. \tag{7}$$

II. Leakage and Nonlinearity

The main idea of rewriting the CM governing equations sketched in section I is to obtain a CM formulation in which each parameter represents a physically motivated quantity in order to distinguish their origin within the electromagnetic field computation. The definition of the armature field ${}^{a}\vec{B}$ in (6) includes an implicit formulation of $\vec{\lambda}$ in the ansatz function of the field ${}^{p}\vec{B}$. For further purposes, $\vec{\lambda}^*$ must be factorized

$${}^{g}\vec{B}^{CM}(I, \psi) = \vec{\lambda}^* \cdot \left(\vec{B}^{CM} + {}^{a}_{u}\vec{B}^{CM}(I, \psi)\right), \tag{8}$$

where an arbitrary permeance state $\vec{\lambda}$ is identical for both field fraction of ${}^{g}\vec{B}^{CM}(I, \psi)$. In (8) the auxiliary field ${}^{a}_{u}\vec{B}^{CM}(I, \psi)$ is defined by

$${}^{a}_{u}\vec{B}^{CM}(I, \psi) = \left(\vec{\lambda}^*\right)^{-1} \cdot {}^{a}\vec{B}^{CM}(I, \psi). \tag{9}$$

A. Ideal Case

The comparative study [7] for modern analytical models for the electromagnetic field prediction concludes that the relative error of the air gap flux density obtained by CM with respect to FE prediction increases strongly in function of the slot-opening to slot-pitch-ratio. In order to analyze this with CM field computation, a PMSM with a slot-opening-factor of 43% is studied. The cross-section of the motor is

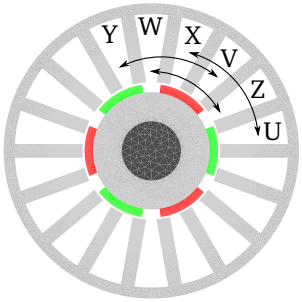

Fig. 1: PMSM Cross-Section

TABLE I: PMSM Parameters

3	Number of Pole Pairs
18	Number of Stator Teeth
0.73	Pole Pitch Factor
3 mm	Permanent Magnet Height
24.5 mm	Rotor Radius (inc. PM)
0.8 mm	Air Gap Height
54.2 mm	Outer Stator Radius
43 %	Slot Opening Factor
1.35 T	Remanence Flux Density
101 mm	Length
4 mm	Yoke Width

depicted in Fig 1. All parameters of the geometry and the electromagnetic evaluation are given in Table I. The torque computation by Maxwell stress theory in case of CM is given in [8]. Figure 2(a) compares the cogging torque in function of rotor position and the corresponding time step obtained by (8) and by a FE computation where the stator is modeled as infinite permeable iron (IFEA), utilizing Neumann boundary condition. One observes that in several rotor positions the torque results are close to each other, but in other angle ranges CM overestimates the integral quantity torque, which is in agreement to the statements of [7]. The maximum deviation occurs at step three, where the edge of the magnet is aligned with the center of the slot. The corresponding flux density distribution, depicted in Fig. 3, shows a significant increase in its tangential component evoked by a flux path deformation in direction of the stator teeth. This effect is also known as slot leakage [9], and cannot be covered by the scalar vector quantity $\vec{\lambda}$ in (4). Adding this effect as optional correction, (8) becomes

$$ {}^{g}\vec{B}^{CM-Mod}\left(I,\psi\right) = \vec{\lambda}^{*} \cdot \left(\vec{B}^{CM} + {}^{a}_{u}\vec{B}^{CM}\left(I,\psi\right) + \Delta\vec{B} \right), \tag{10} $$

where $\Delta\vec{B}$ is the slot leakage of the rotor field. $\Delta\vec{B}$ can be determined by a single IFEA in no-load case. A comparison of the torque results in rated operation in case of IFEA and the application of (8) and (10) shows that the deviation of standard CM vanishes, see Fig. 2(b) and Fig. 3.

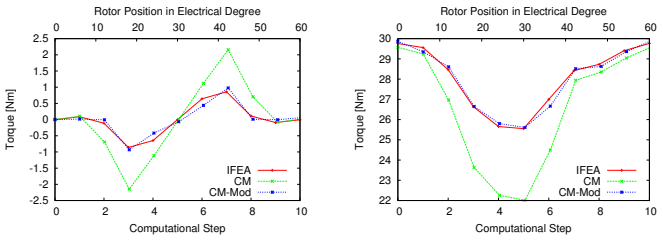

(a) Cogging Torque (b) Torque for $J = 6\frac{A}{mm^2}$.

Fig. 2: Comparison of cogging and rated torque obtained by IFEA, CM and CM-Mod.

B. Nonlinear Case

The formalism in II-A to obtain (10) can also be applied in order to represent saturation. In this case, the permeance state $\vec{\lambda}$ turns from a constant quantity into a function of the magnitude of the current I and the flux weakening angle ψ,

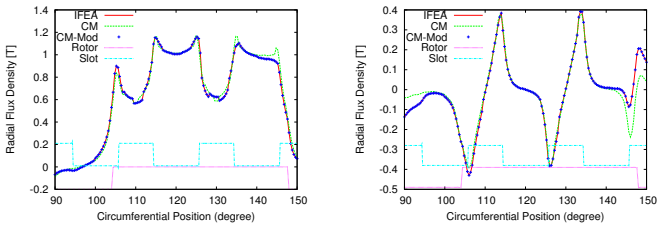

(a) B_r (b) B_φ

Fig. 3: Comparison of radial and tangential flux density obtained by IFEA, CM and CM-Mod in time step three. (Rotor/Slot denote the relative geometry position)

yielding

$$ {}^{g}\vec{B}^{CM}\left(I,\psi\right) = \vec{\lambda}^{*}\left(I,\psi\right) \cdot \left(\vec{B}^{CM} + {}^{a}_{u}\vec{B}^{CM}\left(I,\psi\right) + \Delta\vec{B} \right). \tag{11} $$

For single points of interest, e.g. rated operation, $\vec{\lambda}\left(I,\psi\right)$ can be identified from a single nonlinear FE simulation ${}^{g}\vec{B}^{FEA}\left(I,\psi\right)$ by

$$ \vec{\lambda}\left(I,\psi\right) = \left(\vec{B}^{CM} + {}^{a}_{u}\vec{B}^{CM}\left(I,\psi\right) + \Delta\vec{B} \right)^{-*} \cdot {}^{g}\vec{B}^{FEA}\left(I,\psi\right) \tag{12} $$

to further improve the analytic field computation.

III. Conclusion

In this paper, the standard CM approach is extended to obtain a set of ansatz functions which can each be related to meaningful design quantities, modeling the effect of slotting and slot leakage on the rotor and armature field fraction respectively. This parameters can be re-parameterized by ideal and nonlinear FEA to account for leakage and saturation phenomena. A first demonstration on a load and no-load case of a PMSM yields results which are in good agreement to ideal FEA. The extension procedure to capture nonlinear phenomena is also shown and will be demonstrated on saturated operation points in the full paper.

References

[1] Z. Zhu and D. Howe, "Instantaneous magnetic field distribution in brushless permanent magnet DC motors. III. effect of stator slotting," *Magnetics, IEEE Transactions on*, vol. 29, no. 1, pp. 143–151, 1993.

[2] Z. Zhu, D. Howe, and C. Chan, "Improved analytical model for predicting the magnetic field distribution in brushless permanent-magnet machines," *Magnetics, IEEE Transactions on*, vol. 38, no. 1, pp. 229–238, 2002.

[3] D. C. Hanselman, *Brushless Permanent Magnet Motor Design*, 2nd ed. The Writers' Collective, Mar. 2003.

[4] D. Zarko, D. Ban, and T. Lipo, "Analytical calculation of magnetic field distribution in the slotted air gap of a surface permanent-magnet motor using complex relative air-gap permeance," *Magnetics, IEEE Transactions on*, vol. 42, no. 7, pp. 1828–1837, 2006.

[5] ——, "Analytical solution for cogging torque in surface Permanent-Magnet motors using conformal mapping," *Magnetics, IEEE Transactions on*, vol. 44, no. 1, pp. 52–65, 2008.

[6] K. J. Binns, *Analysis and computaion of electric and magnetic field problems,.* Pergamon Press; [distributed in the Western Hemisphere by Macmillan, New York], 1963.

[7] L. Wu, Z. Zhu, D. Staton, M. Popescu, and D. Hawkins, "Comparison of analytical models for predicting cogging torque in surface-mounted PM machines," in *Electrical Machines (ICEM), 2010 XIX International Conference on*, 2010, pp. 1–6.

[8] M. Hafner, D. Franck, and K. Hameyer, "Static electromagnetic field computation by conformal mapping in permanent magnet synchronous machines," *Magnetics, IEEE Transactions on*, vol. 46, no. 8, pp. 3105–3108, 2010. [Online]. Available: 10.1109/TMAG.2010.2043930

[9] K. Oberretl, "Die Berechnung des Streuflusses im Luftspalt von elektrischen Maschinen mit Käfig- oder Dämpferwicklungen Teil 1: Theorie und Berechnungsmethoden," *Archiv fur Elektrotechnik Berlin*, vol. 69, no. 1, pp. 11–22, 1986, compendex.